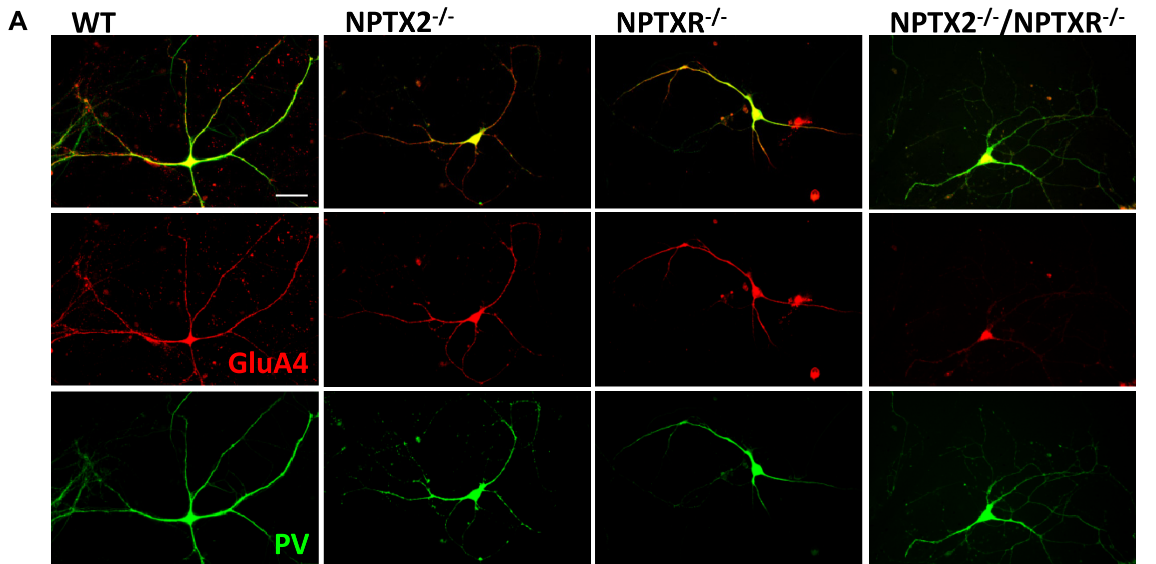

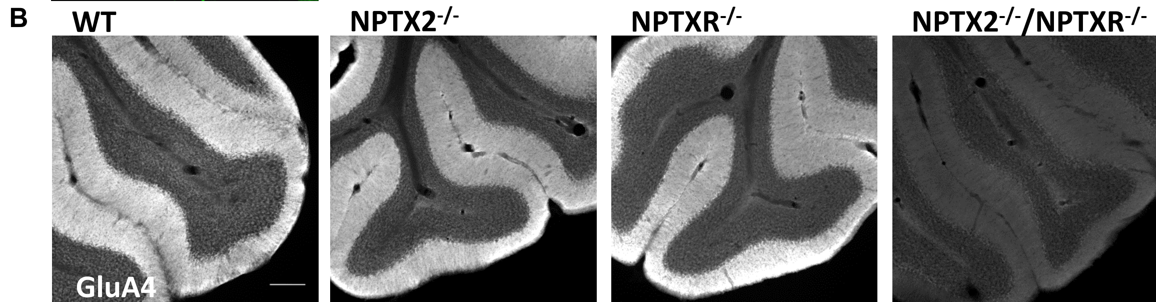

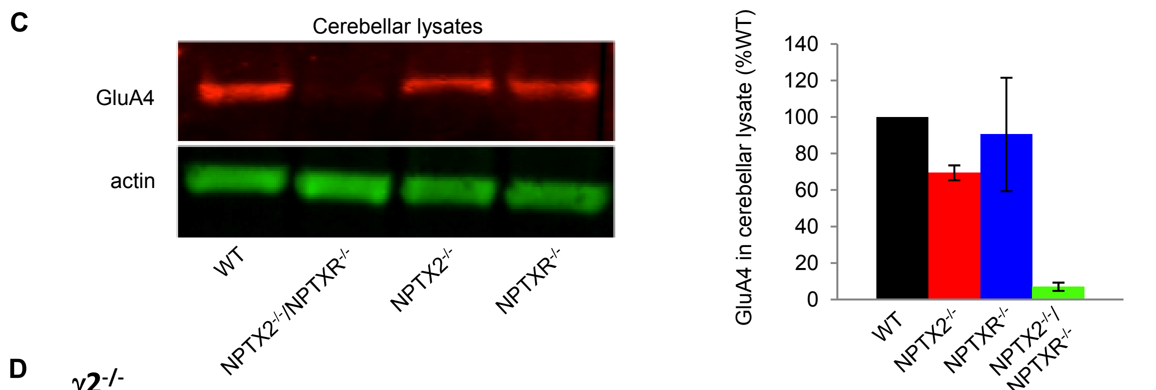

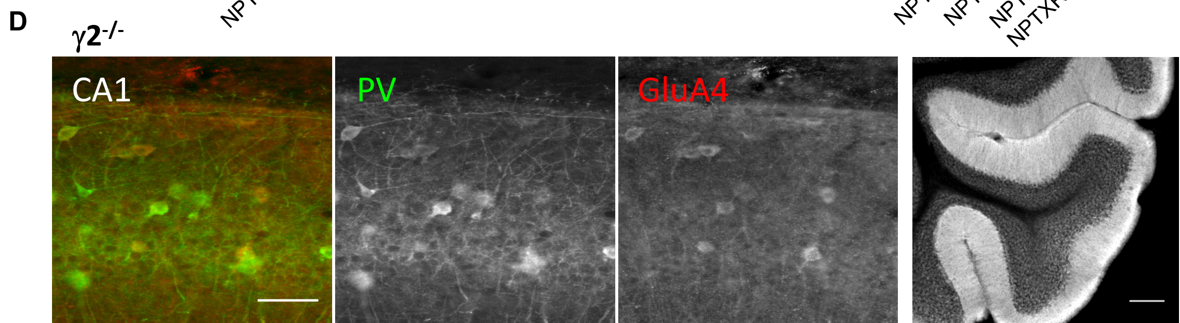

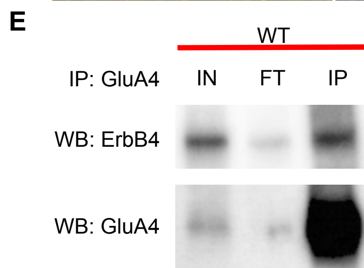

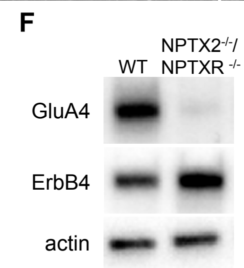

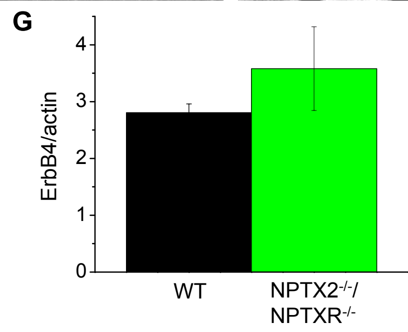

Supplemental Fig. 1

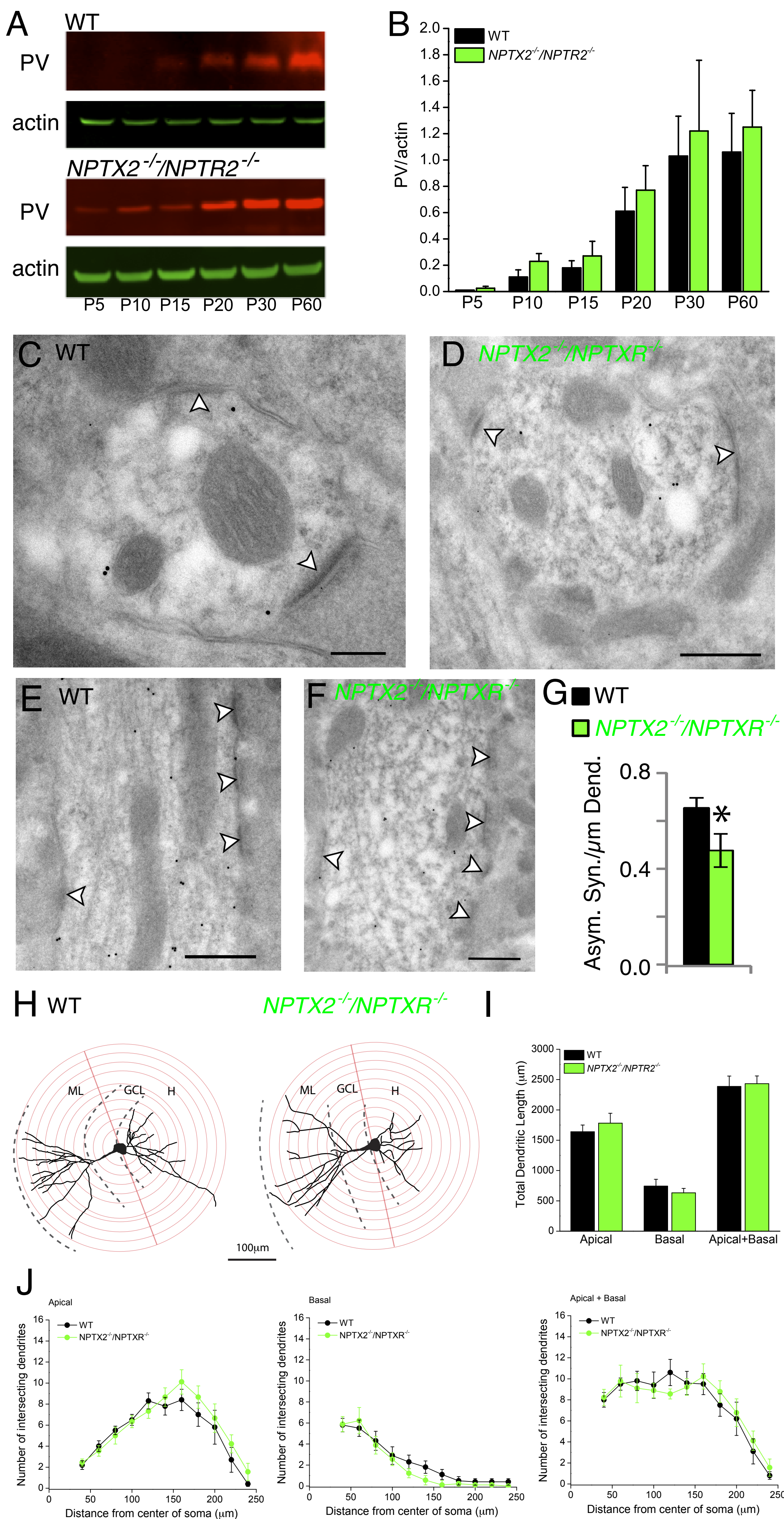

Supplemental Fig. 2

Supplemental Figure 1 (related to Figures 2 and 3): Loss of GluA4 in *NPTX2$^{-/-}$/NPTXR$^{-/-}$* mice but not stargazin$^{-/-}$ mice and normal ErB4 levels in *NPTX2$^{-/-}$/NPTXR$^{-/-}$* mice.

(A) Images of representative PV+ cells in hippocampal cultures from wild type, *NPTX2$^{-/-}$*, *NPTXR$^{-/-}$*, *NPTX2$^{-/-}$/NPTXR$^{-/-}$* mice illustrating co-localization of GluA4 (scale bar, 50 microns). (**B**) Images of representative cerebellar sections from wild type, *NPTX2$^{-/-}$*, *NPTXR$^{-/-}$*, *NPTX2$^{-/-}$/NPTXR$^{-/-}$* mice stained for GluA4 (bar, 200 microns). (**C**) At left are representative sample western blots from cerebellar lysates of wild type, *NPTX2$^{-/-}$*, *NPTXR$^{-/-}$*, *NPTX2$^{-/-}$/NPTXR$^{-/-}$* mice probed for GluA4 (above) and beta actin (below) content. At right is the quantitative summary of GluA4 levels in cerebellar lysates from *NPTX2$^{-/-}$*, *NPTXR$^{-/-}$*, *NPTX2$^{-/-}$/NPTXR$^{-/-}$* mice relative to paired wild type controls. For each NPTX genotype GluA4/B-actin ratio is expressed as a percentage of the GluA4/B-actin ratio measured in paired wild type cerebellar lysates. A total of 4 mice from 4 independent litters for each genotype were paired and analyzed in parallel. Values are average±s.e.m. (**D**) Representative sample images of PV and GluA4 staining in a CA1 hippocampal section from a stargazin$^{-/-}$ mouse (first 3 panels, bar is 50 microns). Also shown is a representative sample image of GluA4 expression in a cerebellar section from a stargazin$^{-/-}$ mouse (4th panel, bar is 200 μm). (**E**) Representative immunoblots illustrating that pull-down of GluA4 from hippocampal synaptic plasma membranes co-precipitates ErbB4 as well as GluA4 itself (IP lanes). Also shown are the input (IN) and flow through (FT) materials probed with the same antibodies (note that these blots come from the same sample probed for stargazin in figure 3E of the manuscript). (**F**) Representative western blots of SPM fractions from wild type and *NPTX2$^{-/-}$/NPTXR$^{-/-}$* hippocampi probed for GluA4, ErbB4, and actin as indicated (note that these blots are from the sample shown in figure 2J of the manuscript). (**G**) Histogram summarizing the levels of ErbB4 relative to actin in hippocampal SPM fractions from wild type and *NPTX2$^{-/-}$*

/NPTXR$^{-/-}$ mice. A total of 3 mice from 3 different litters for each genotype were paired, processed, and analyzed in parallel.

Supplemental Figure 2 (related to Figure 4): PV levels, PVFSI synapse density, and PVFI dendritic architecture in wild type and *NPTX2*$^{-/-}$*/NPTXR*$^{-/-}$ mice.

(**A**) Representative sample immunoblots of hippocampal lysates from wild type (upper) and *NPTX2*$^{-/-}$*/NPTXR*$^{-/-}$ mice (lower) probed for PV and actin at the developmental ages indicated. (**B**) Group data summary of hippocampal PV levels (normalized to actin) through development in wild type and *NPTX2*$^{-/-}$*/NPTXR*$^{-/-}$ mice. A total of 3 mice for each genotype were examined in parallel at each developmental time point. (**C-F**) Sample electron micrographs from wild type and *NPTX2*$^{-/-}$*/NPTXR*$^{-/-}$ mice as indicated illustrating assymetric synapses (arrowheads) onto hippocampal PV decorated (15 nm gold) dendrites (scale bars = 200 nm (F), 500 nm (C-E)). (**G**) Histogram summarizing the density of asymmetric synapses onto PV-labeled dendrites in wild type and *NPTX2*$^{-/-}$*/NPTXR*$^{-/-}$ mice. A total of 185 μm of PV decorated dendritic profiles in 52 sections from 2 wild type mice and 141 μm of PV labeled dendritic profiles from 31 sections from 3 *NPTX2*$^{-/-}$*/NPTXR*$^{-/-}$ mice were examined (* $p<0.05$, Kruskal-Wallis test). (**H**) Representative single examples of the dendritic arborizations from post-hoc identified wild type and *NPTX2*$^{-/-}$*/NPTXR*$^{-/-}$ dentate gyrus PVFSIs. Concentric circles for subsequent Sholl analyses were constructed as shown (red circles); ML- molecular layer, GCL- granule cell layer, H- hilar region. (**I**) Histogram summary of the total length for apical, basal, and apical+basal dendrites for dentate gyrus PVFSIs from WT (black bars, n=10) and NPTX2$^{-/-}$/NPTXR$^{-/-}$ (green bars, n=9) mice. (**J**) Plots of total number of intersecting dendrites at each concentric circle shown in **H** for apical (left panel), basal (middle panel) and apical+basal (right panel) for WT (black; n=10) and NPTX2$^{-/-}$/NPTXR$^{-/-}$ (green, n=9) mice.

Materials and Methods

Animals

All experiments were conducted in accordance with animal protocols approved by the NIH. Male and female wild type, *NPTX2*$^{-/-}$, *NPTXR*$^{-/-}$, *NPTX2*$^{-/-}$/*NPTXR*$^{-/-}$, *Nkx2-1-cre*:RCE and *Nkx2-1-cre*:tdTOM reporter mice were used as indicated. Breeding and genotyping of *Nkx2-1-cre* mice was performed as previously described (Tricoire et al., 2010). Genotyping for *NPTX2*$^{-/-}$, *NPTXR*$^{-/-}$, and *NPTX2*$^{-/-}$/*NPTXR*$^{-/-}$ mice was performed by PCR with the following primers: *NPTX2* forward ctcggtcaaggatttctcagc, *NPTX2* reverse cgcgctctctgattggtc, and *NPTX2* mutant reverse tctctcgtgggatcattgttt; *NPTXR* forward gcctgaagaacgagatcagc, *NPTXR* reverse agagggcctacaagctgtca, and *NPTXR* mutant reverse cagcagatggccttctagtt. Double homozygotes were crossed for litter production. Stargazin$^{-/-}$ mice were generously provided by Dr. Katherine Roche's lab at the NIH.

IHC

Hippocampal sections. In all instances except postnatal day 2 (P2) time points, mice were anesthetized with isofluorane and transcardially perfused with 1X PBS followed by 4% PFA. Brains were removed and post-fixed overnight in 4% PFA at 4°C. For P2, pups were decapitated and the heads fixed overnight in 4% PFA at 4°C, after which brains were removed. Brains were cryoprotected in 30% sucrose in PBS. P2 and P5 brains were embedded in Tissue Freezing Medium (Triangle Biomedical Sciences, North Carolina), frozen on dry ice, and sectioned via cryostat (20-30µm) directly onto gelatin-coated slides. All other brains were sectioned on a freezing microtome (45µm) and stored in PBS at 4°C.

For immunoperoxidase labeling, floating cryosections of P19-P60 mouse brains were blocked for 3h in NGS solution with 1% triton using an avidin biotin kit (Vector Labs, California), then incubated for two days in guinea pig anti-GluA4N (1:2000, Frontier Science, Japan) at room temperature. Sections were incubated in secondary (1:500, Vector Labs, California), processed with an ABC Kit (Vector Labs, California), developed in stable diaminobenzidine (Life Technologies, New York) and treated with 1% osmium tetroxide before dehydration and mounting.

For immunofluorescent staining, all sections were washed with 1X PBS then blocked for 2 hr at room temperature in PBS/0.5% Triton X-100/1% BSA/10% normal goat serum (NGS) solution before incubation overnight at 4°C with primary antibodies diluted in PBS/0.5% Triton X-100/1% BSA/1% NGS (BGT-PBS). Primary antibodies were: rabbit anti-GluA4 (1:150; Millipore, Massachusetts), mouse anti-parvalbumin (1:1000; SWANT, Switzerland), chicken anti-GFP (1:2000; Aves Labs, Oregon) and biotinylated Wisteria Floribunda Lectin (1:500; Vector Labs, California). Sections were washed 4 X 15 min in BGT-PBS, then incubated (1hr/room temperature) in secondary antibody diluted in BGT-PBS. Secondary antibodies were: goat anti-rabbit AlexaFluor488 and 555, goat anti-mouse AlexaFluor555, goat anti-chicken AlexaFluor488 and streptavidin, AlexaFluor633 conjugated (all 1:1000; Molecular Probes, New York). Sections were washed in BGT-PBS, free-floating sections were mounted on gelatin-coated microscope slides, and all slides were coverslipped in Vectashield Hard Set Mounting Medium with DAPI (Vector Labs, California). Images were captured on an Olympus AX70 microscope, using a Retiga 4000R cooled CCD camera with QCapture Suite (Qimaging, British Columbia), or on an LSM 510 confocal microscope (Zeiss, Germany). Labeled cells were manually counted using the cell-counter plugin of ImageJ software (NIH, Maryland). For

density measurements, the surface area of the region of interest was measured in ImageJ then multiplied by the slice thickness to yield cells/mm^3.

Cell cultures. P0- pups (5/litter) were anesthetized with isofluorane, decapitated, and their brains dissected into Simple D1 (SD1; HBSS (no Mg^{2+} or Ca^{2+}) with 10mM HEPES, 1mM sodium pyruvate and 100U/ml penicillin/streptomycin). Hippocampi were isolated in ice cold SD1, then digested and dissociated using the Worthington Papain Dissociation System (Worthington Corporation, New Jersey). Dissociated cells were diluted to 10^5 cells/ml in Plating Medium (PM; Neurobasal-A Medium supplemented with B27, 0.5mM L-Glutamine, 5% fetal bovine serum, 25μM glutamic acid and 100U/ml penicillin/streptomycin). $5x10^4$ cells (0.5ml suspension) were plated on poly-D-lysine coated 12mm coverslips (BD Biosciences, California) in 24-well plates and incubated at 37°C, 95% O_2/5% CO_2, 4 hours to overnight. Half the PM was removed and replaced with Neurobasal-A Medium supplemented with B27, 0.5mM L-Glutamine and bFGF (10ng/ml). Medium was changed every 3-5 days thereafter, and 5μM cytosine arabinoside was added at 3 days in vitro (DIV3) for 48 hours to inhibit glial proliferation. DIV15 to DIV30 cultures were used for immunocytochemistry. Cells were fixed in 4% paraformaldehyde at room temperature for 15min and permeablized with 0.2% Triton X-100 in 1X PBS for 10min, then blocked with 10% NGS in 1X PBS for 30min. Cells were incubated with primary antibodies (rabbit anti-GluR4 (1:250; Millipore), mouse anti-parvalbumin (1:3000; SWANT), or rabbit anti-Stargazin (1:500; Millipore) diluted in 1X PBS for 1 hour at room temperature. Secondary antibodies (goat anti-mouse Alexa Fluor 488 and goat anti-rabbit Alexa Fluor 555, Molecular Probes) were diluted 1:1000 in 1X PBS and incubated with cells at room temperature for 30min. Coverslips were mounted using Vectashield Hard Set Mounting Medium with DAPI.

Post-embedding electron microscopy

Mice (2 months old) were perfused through the ascending aorta with 4% PFA+0.5% glutaraldehyde and processed as reported in (Petralia and Wenthold, 1999). Post-fixed and rinsed brains were sectioned at 350 µm on a vibratome, the hippocampus was isolated, cryoprotected, frozen in liquid propane, immersed in 1.5% uranyl acetate in methanol at -90°C, infiltrated with Lowicryl HM 20 resin at -45°C and polymerized with UV light. Dark yellow ultramicrotome sections (~80 nm) were collected on grids, labeled with rabbit anti-parvalbumin (1:50, Frontier Science Af750) and guinea pig anti-GluA4N (1:25, Frontier Science Af640), followed by 15 and 5 nm gold secondaries (1:40), counterstained and examined on a JEOL 2100 electron microscope.

To determine synaptic density of GluA4 labeling, the length of asymmetric synapses on parvalbumin-labeled dendrites in radiatum was measured in Image J, and GluA4-labeled immunogold particles were counted in the postsynaptic density or within 25 nm of the postsynaptic membrane (to allow for the length of the antibody against the extracellular N-terminus). Individual synaptic densities for each genotype were combined, and significance determined by the Mann-Whitney U Test using IBM SPSS Statistics 21. Measurements for the density of asymmetric synapses on parvalbumin-labeled dendrites were done in Image J, and significance ascertained with the Kruskal-Wallis Test.

Western blot, Fractionation, and Immunoprecipitation

For Western blot analysis, P30 mice were anesthetized with isofluorane, decapitated, and the brains removed. For hippocampal synaptosomal preparations hippocampi were isolated in ice cold 1XPBS and then for each hippocampus, 250ul Syn-PER(ThermoScientific) plus protease

inhibitors were added and transferred to a Dounce tissue grinder on ice. Homogenization was performed on ice in the Dounce grinder with 10 slow strokes and homogenate was centrifuged at 1200xg at 4°C for 10minutes. Supernatant was then collected and centrifuged at 15,000xg at 4°C for 20minutes. The resulting pellet was suspended in THMB+1% TritonX100+Protease inhibitors at 100ul/hippocampus and protein quantity was measured using BCA (ThermoScientific). For cerebellar lysates cerebella were removed into pre-chilled THMB: 25mM TrisHCl, pH 7.4, 150mM NaCl, 2 mM EDTA and 10 µl/ml Halt Protease Inhibitor (ThermoScientific, Massachusetts). Tissue was mechanically homogenized then sonicated for 5 x 3sec. Triton X-100 was added to 1% of the volume and the homogenate was incubated on ice for 1hr. The homogenate was centrifuged at 14,000 rpm at 4°C for 15min, lysate was collected and used in BCA assays to determine protein concentration. For both hippocampal and cerebellar preps, 40 µg of protein was loaded per lane onto 3-8% Tris-Acetate mini gels (Life Technologies, New York) and separated by electrophoresis for 1h at 100V. Gels were transferred to PVDF membranes using the iBlot system (Life technologies). Blots were blocked in Odyssey Blocking Buffer (LI-COR, Nebraska) and probed for GluA4 (rabbit anti-GluA4, 1:500, Millipore); beta-actin (mouse anti-beta-actin, 1:5000, abcam) was used as the standard. Secondary antibodies were: IRDye 680 goat anti-rabbit (1:15000, LI-COR) and IRDye 800 goat anti-mouse (1:15000, LI-COR). Blots were scanned using Odyssey Classic Infrared Imaging System (LI-COR). Fluorescent bands were quantified using Image Studio software.

Hippocampal membrane fractionation. Membrane fractionation was performed essentially as described by (Gray and Whittaker, 1962). Briefly, WT or *NPTX2*$^{-/-}$/*NPTXR*$^{-/-}$ mice were isoflurane anesthetized, rapidly decapitated and brains transferred to a petri dish containing ice cold HEPES-buffered sucrose (HBS, 320mM sucrose, 4mM HEPES and protease inhibitors

(Roche)). Hippocampi where carefully isolated from cortex under a dissecting microscope and then mechanically disrupted with a Dounce-type homogenizer. Pooled (4 mice/8 hippocampi) homogenized membranes where diluted to 10 wt/vols, centrifuged at 1kxg for 10min at 4°C to remove nuclei and cellular debris, re-equilibrated to initial volume in HBS and subjected a second round of centrifugation at 17kxg for 30min @ 4°C. The resulting crude membrane fraction was washed, exposed to hypo-osmotic shock and pooled membranes resuspended in HBS. Membranes were layered onto a discontinuous sucrose gradient consisting of 1.2, 1, 0.8M sucrose, all in 4mM HEPES with protease inhibitors, and spun at 150kxg for 2h at 4°C. The flocculent membrane fraction at the 0.32/0.8M interface is referred to as light membranes (LM), the layer at the 0.8/1.0M interface as mixed membranes (MM) and the 1.0/1.2M as synaptic plasma membranes (SPM).

Immunoprecipitation of GluA4 from Hippocampal SPM. Immunoprecipitations were performed essentially as described (Mitchell et al., 2013). Briefly, SPM was solubilized by the addition of 1% TritonX-100 @4°C under constant agitation for 30min. Unsolubilized membranes where cleared by centrifugation at 5kxg for 5min. Solubilized membranes were diluted to 1mg/mL total protein in PBS with 1% TritonX-100 and protease inhibitors maintained at 4°C. Rabbit anti-GluA4 affinity purified polyclonal antibody (Chemicon 1508, Millipore) was pre-conjugated to Protein-A Plus agarose beads (Pierce) at a ratio of 10μg antibody/20uL bead slurry in PBS at room temp for 1h. Immunoprecipitation was performed @10ug antibody/mg protein (typically between 250-500μg solubilized protein) under gentle agitation at 4°C for at least 3h or overnight. A small amount of reaction fractions (input, IN and flowthrough, FT) were used to make LDS samples and determine the efficiency of IP. Samples were reduced by addition of 5% BME (Sigma) @80°C for 10min. Following extensive washes in the IP buffer, bound protein was

eluted with 1.5X LDS sample buffer and all fractions where resolved by SDS-PAGE, transferred to nitrocellulose, blocked and incubated with appropriate antibodies. Protein bands where visualized with ECL and images acquired with a ChemiDoc gel imager (BioRad). For densitometeric analysis of GluA4 & ErbB4 Image lab 4.1 was used.

Real-time RT-PCR

Hippocampi from P20 wild type and *NPTX2*$^{-/-}$/*NPTXR*$^{-/-}$ mice were isolated. Total RNA were prepared using RNAqueos-4PCR kit (Life Technologies Corp.). cDNA was generated using High Capacity RNA-to-cDNA kit (Applied Biosystems). Yield was estimated using both spectrophotometry as single strand DNA and agarose gel electrophoresis in comparison to DNA standards. Quantitative PCR was carried out using a StepOne instrument from Applied Biosystems. Comparative C_T experiments were designed and setup using Design Wizard software (Applied Biosystems). cDNAs from wild type and *NPTX2*$^{-/-}$/*NPTXR*$^{-/-}$ hippocampi were used at 100ng for each 20 µl reaction. PV and GluA4 were targeted using FAM-Gria4 (Mm00444754-ml, Applied Biosystems) and FAM-Pvalb (Mm00443100-ml, Applied Biosystems) respectively. VIC-Gapdh (Mm9999915, Applied Biosystems) was used as an endogenous control. Real-time PCR was run under the thermal profile: 50°C, 2 min; 95°C, 10 min; 50 cycles of (95°C, 15 s; 60°C, 1 min). 3 independent real-time PCR experiments were performed using RNA prepared from independent mouse brains from independent litters. In each PCR, 3 replicates were run for each sample/target. PCR analysis was performed using the StepOne software (Applied Biosystems). Cycle threshold (C_T) for each targeted gene was normalized to the C_T of the endogenous control gene gapdh to obtain the ΔC_T values. The relative abundance of a targeted gene within the sample in relation to gapdh is calculated as $2^{\Delta CT}$.

Fluorescent *in situ* hybridization

Wild type and $NPTX2^{-/-}$/$NPTXR^{-/-}$ mice were deeply anesthetized with isofluorane and sacrificed by cervical dislocation. Brains were removed and frozen in crushed dry ice for 5 min, then stored at -80° C until sectioning. Fresh frozen sections (10 µm) were used for double fluorescent *in situ* hybridization (FISH) using the manufacturer's protocol for fixation, protease treatment, probe hybridization, preamplification, amplification and fluorescent detection (RNAscope® Fluorescent Multiplex Kit, Advanced Cell Diagnostics Inc., Hayward, CA). Briefly, 20 sets of "ZZ" probe pairs were designed for each target RNA species, with binding sequences for both the target RNA and a preamplifier on each "Z." Binding of both "Z's" in a pair to the RNA is necessary in order to form the full preamplifier binding site. The 20 preamplifiers each bind 20 amplifiers, each of which in turn binds 20 fluorescent label probes. This sequential amplification scheme enables visualization of single RNA molecules. Probes were designed against a ~1kb region spanning bases 2-885 in parvalbumin (PV) and 454-1514 in Gria4. For double FISH, unique fluorophores were used to detect signals from the PV and Gria4 probes; DAPI was used to label cell nuclei. In control experiments using probes against DapB, an *Escherichia coli* protein not found in mammalian tissue, no signal was detected. 10x DAPI images and 40x FISH images were acquired with an Olympus Provis AX70 microscope using a Retiga 4000R cooled CCD camera and the QCapture Suite (Qimaging, British Columbia).

Slice Electrophysiology

Hippocampal slices (300-350µm thick) were prepared from P5 to P30 wild type, *$NPTX2^{-/-}$*, *$NPTXR^{-/-}$*, *$NPTX2^{-/-}$/$NPTXR^{-/-}$* mice as indicated. Mice were anesthetized with isoflurane, and the brain was dissected in ice-cold saline solution (in mM): 130 NaCl, 24 $NaHCO_3$, 3.5 KCl, 1.25 NaH_2PO_4, 1 $CaCl_2$, 5.0 $MgCl_2$, and 10 glucose, saturated with 95% O_2 and 5% CO_2, pH 7.4.

Transverse slices were cut using a VT-1000S vibratome (Leica Microsystems, Bannockburn, IL) and incubated in the above solution at 35˚C for 30min then kept at room temperature until use. Slices were transferred to a recording chamber and perfused (3-5ml/min, 32-35˚C) with artificial cerebrospinal fluid (ACSF; in mM): 130 NaCl, 24 $NaHCO_3$, 3.5 KCl, 1.25 NaH_2PO4, 2.5 $CaCl_2$, 1.5 $MgCl_2$, 10 glucose, (supplemented with 0.1 ± dl-AP5, 0.02 DNQX, and/or 0.005 bicuculline methobromide as needed) saturated with 95% O_2/5% CO_2, pH 7.4. Putative PVFSIs in the dentate gyrus, and CA1 pyramidal cells, visually identified using IR-DIC video microscopy (Zeiss Axioskop) were targeted for whole-cell recording using a multiclamp 700A amplifier (Axon Instruments, Foster City, CA). Recording electrodes (3-5MΩ) pulled from borosilicate glass (WPI, Sarosota, FL) were filled with one of two intracellular solutions (in mM): 1) 130 K-gluconate, 5 KCl, 0.6 EGTA, 2 $MgCl_2$, 2 Na_2ATP, 0.3 GTPNa, and 10 HEPES, pH 7.2-7.3, 290mOsm for sEPSC and intrinsic electrical property recordings; 2) 100 Cs-gluconate, 5 CsCl, 0.6 EGTA, 5 $MgCl_2$, 2 Na_2ATP, 0.3 GTPNa, 40 HEPES, 0.1 spermine, and 1 QX-314, pH 7.2-7.3, 290mOsm for evoked synaptic and GDP recordings. Biocytin (0.2%) was added to the intracellular solution for *post hoc* morphological processing of recorded cells to confirm basket cell anatomy using fluorescently conjugated avidin. Uncompensated series resistance, 5-15 MΩ, was rigorously monitored and recordings were discarded if changes >10% occurred. Data acquisition and analysis were performed with pClamp 9.2 (Axon Instruments, Foster City, CA). Firing properties were monitored in current-clamp by delivery of electrotonic current injections with the resting membrane potential biased to -60 mV, and sEPSC were monitored in voltage-clamp at a holding potential of -60mV. All cells included in the PVFSI group for analysis exhibited fast spiking and/or basket cell anatomy. sEPSCs were detected and analyzed in Clampfit using a template event detection strategy for 30s of gap-free recording. For each cell,

all events collected were averaged and this average sEPSC was used to determine the amplitude, 10-90% rise time, and decay time constant (monoexponential fit). Synaptic events were evoked by low-intensity stimulation (150μs/10–30μA) in the granule cell layer (for mossy fiber inputs), middle molecular layer (for medial perforant path inputs), or CA1 stratum radiatum (for Schaffer collateral inputs) via a constant current isolation unit (A360, WPI) connected to a patch electrode filled with oxygenated ACSF. GDPs were assayed for a minimum of 15 minutes by recording CA1 PCs voltage-clamped at a holding potential of 0 mV (reversal potential for glutamatergic synaptic events) with no synaptic blockers in the bath. In this configuration GDPs were observed as regularly occurring GABA-mediated (bicuculline sensitive, data not shown), multi-peaked outward currents with a minimum half-width and total duration of 105 and 500 ms respectively, making them easy to separate from spontaneous unitary IPSCs. GDPs were detected offline using a threshold detection algorithm and subsequent visual inspection of individual events.

For gamma oscillation experiments, following dissection slices were placed into an interface-style chamber (Warner Instruments, CT) containing humidified carbogen gas and perfused (1-1.5ml/min, 34°C) with modified ACSF (in mM): NaCl (126), KCl (3), $MgCl_2$ (2), $CaCl_2$ (2), NaH_2PO_4 (1.25), glucose (10) and $NaHCO_3$ (26) saturated with 95% O_2 and 5% CO_2. Slices were incubated for at least 1h before recording. Field potentials were recorded from CA3 using glass pipettes (3–5MΩ) filled with ACSF. Signals were low-pass filtered at 2kHz and acquired at 10kHz using an Axopatch1D (Molecular Devices, CA), digitized using a Digidata1322A (Molecular Devices, CA) and captured on a computer running pClamp9 (Molecular Devices, CA). Gamma oscillations were induced by 25μM carbachol (Sigma-Aldrich, MO). Data were imported into Igor Pro (Wavemetrics, OR) using NeuroMatic

(ThinkRandom, UK) and analysed using custom-written procedures. Gamma power was calculated using 2min bins for recordings of at least 30min; gamma frequency was calculated as the average frequency across all bins and peak gamma power was taken from the maximum observed during the recording. Example traces show either the local field potential (band-pass filtered between 30-120Hz) or Wavelet transforms of the unfiltered traces.

For epileptiform circuit activity all recordings were carried out in interface conditions as described above. After recording baseline activity for at least 10 minutes, epileptiform activity was induced by increasing the extracellular K^+ concentration to 8.5 mM (Traynelis and Dingledine, 1988). This high-potassium model replicates the main electrical features of epilepsy, including interictal bursts and ictal events containing both tonic and clonic components. Epileptiform activity was recorded simultaneously from CA3 and CA1 with both ictal and interictal events being evident at both recording locations. However, at this developmental stage in mice CA3 recordings yielded more robust epileptiform discharges, so recordings from the CA3 electrode were used for further analyses. Ictal and interictal events were detected and separated automatically using custom-written procedures in Igor Pro as follows. First, traces were high-pass filtered at 5 Hz to remove any DC drift from the recordings. The RMS of the entire recording was then calculated, and our detection algorithm detected ictal and interictal events as threshold crossings (typically 10 to 20x the average value of the transformed trace during the baseline period). Interictal events were detected as threshold crossings of at least 15 ms duration, occurring at an inter-event interval of at least 400 ms (typical interictal event frequencies were < 1Hz). Ictal events were detected as an initial threshold crossing with the same parameters as interictal event, but followed by at least 10 bursts with an inter-event interval of less than 400 ms (the ‘clonic phase’ of the ictal event). This algorithm reliably separated ictal

and interictal events in our recordings, and all detected events were confirmed by visual inspection.

Statistical analyses were carried out using GraphPad Prism (GraphPad, CA) or OriginPo (Origin Lab, MA). Data were tested for normality using Shapiro Wilk or D'Agostino and Pearson normality tests and then analyzed using either one-way ANOVA or Kruskal-Wallis tests as appropriate. When a significant interaction between groups was detected *post hoc* comparisons were performed using Bonferroni multiple comparisons, Dunn's multiple comparisons, Student's *t*-tests, or Mann-Whitney U tests as indicated. Two tailed paired *t*-tests or Wilcoxon tests were performed where indicated. All values represent mean ± SEM.

PVFSI Dendritic Architecture Analysis

Total dendritic length and Sholl analysis on post-hoc biocytin-filled dentate gyrus basket cells from wild type and NPTX2$^{-/-}$/NPTXR$^{-/-}$ mice were performed using the Simple Neurite Tracer plugin for Fiji (http://fiji.sc/Welcome). For Sholl analyses, concentric circles starting 40μm from the center of the cell body, each 20μm apart, were constructed. The number of intersecting dendrites for each concentric circle was measured and plotted against radial distance from the center of the soma. All analyses were performed blind with respect to the genotype of the mice.

***In vivo* Electrophysiology**

All procedures are consistent with National Institutes of Health guidelines and were approved by The George Washington University Institutional Animal Care and Use Committee. Surgical and recording methods were as described previously (Colonnese and Khazipov, 2010). Briefly, age matched (32-34 days old) wild type and *NPTX2*$^{-/-}$/*NPTXR*$^{-/-}$ mice of both sexes were anaesthetized with isoflurane (5% induction, 1 to 3% maintenance) and, after cleaning the skull,

plastic bars were placed over the occipital and nasal bones and fixed in place with dental cement. Carprofen (5 mg/kg) was used perioperatively as an analgesic, and mice recovered for 2-3 days. For recording, isoflurane-anaesthetised mice were transferred to a modified stereotaxic frame attached to the head fixation apparatus. Body temperature was monitored with a thermocouple placed under the abdomen and maintained at 33 – 36 °C throughout the procedure. Movement was detected using a piezo-based detector placed under the mouse. A craniotomy was made to target CA1 (2.11mm caudal, 1.6mm lateral to bregma) and extracellular recordings were made using a 32 channel multi-site polytrode (Poly2, Neuronexus, Ann Arbor MI) with an electrode separation of 50 μm. The polytrode was inserted to a depth such that the tip was 300 μm below the pyramidal cell layer. The local field potential (LFP) was sampled at 32 kHz and digitized using a Cheetah (Neuralynx) digitizer and software package. Mice were allowed to recover from isoflurane anaesthesia for at least 10 mins before recording to allow collection of data during awake states.

All recordings were down-sampled to 1 kHz and imported into Igor Pro (Wavemetrics) for analysis using custom-written procedures. Power spectra of the unfiltered LFPs were dominated by a large theta component, so were normalized by 1/f to allow analysis and visualization of higher-frequency components. To compare theta and gamma oscillations across strains, individual power spectra were normalized between 0 and 300Hz to calculate the z-score. SWRs were examined during periods of quiet wakefulness, and were automatically detected using methods adapted from those described elsewhere (Csicsvari et al., 1999). Briefly, extracellular recordings were digitally band-pass filtered between 130 and 250 Hz to reveal SWRs, and the root mean square (RMS) of the filtered recording was used for automatic detection. Periods where the RMS crossed a threshold of 7 SDs above the background were

counted as SWR events in our detection algorithm. The nearest peak to the threshold crossing was considered the centre of the SWR and 100 ms on either side of the peak was extracted and transformed using a Morlet wavelet function. The boundaries of the SWRs were defined as 2 SDs above the baseline power (taken from the first 50 ms at 250 Hz) of the wavelet function. The peak power and frequency of the SWR were taken from the wavelet transform, and the amplitude calculated by the peak-to-trough amplitude of the band-pass filtered trace. The RMS of the filtered trace was calculated using the SWR boundaries detected from the Wavelet transform, and those events with an average RMS of less than 4 SDs above the background were rejected.

Behavioral Testing

For behavioral testing we used adult NPTX2$^{-/-}$/NPTXR$^{-/-}$ (n=15), wild-type (n=7) and C57Bl/6J controls (n=8) (The Jackson Laboratory, Bar Harbor, ME) age 10-13 weeks at start of testing. All behavior tests where conducted during the light phase (lights on 0600). Novelty-induced locomotor activity was assessed in a novel square arena (40 x 40 x 35 cm, 55 lux) constructed of white Plexiglas as previously described (Karlsson et al.). The mouse was placed in the arena and left to explore freely for 60 min, which was video recorded and distance traveled and time spent in the center (20 x 20 cm) during the first 10 min were analyzed with "Top Scan" software (Clever Systems, Reston, VA). Anxiety-like behavior was further tested in the elevated O-maze, which consisted of a grey circular path (runway width 5.5 cm, diameter = 57 cm) with 2 opposing compartments protected with walls (height = 12 cm and two open sectors of equal size). The maze was elevated 50 cm above the ground and illuminated from the top (25 lux). At the start of a session mice were placed in one of the two closed arms facing the open arm and allowed to freely explore the apparatus for 5 min. The entire session was video recorded and

analyzed with “Top Scan” software (Clever Systems, Reston, VA). Rewarded alternation on the T-maze, spatial working memory test (non-matching to place) was carried out using a clear Plexiglas T-maze, placed on a white table. The maze consisted of a start arm (31 cm) and two identical goal arms (30 cm), surrounded by a 12.5 cm high wall. Prior to testing, mice were food restricted to 85-90% of their free-feeding weight and habituated to the maze, and to the 50% sweetened condensed milk reward (diluted with water) over several days before rewarded spatial alternation testing began. Each trial consisted of a sample run and a choice run. At the start of each trial, 0.1 ml of the diluted sweetened condensed milk reward was placed in the food wells at the end of each goal arm. On sample runs, the mouse was forced either left or right by blocking access to one goal arm with a clear Plexiglas door according to a pseudorandom sequence. During the choice run, mice were given a free choice of either goal arm. A trial was scored as ‘correct’ if the mouse entered the previously unvisited arm. The delay between sample run and choice run was 10-15s. Mice were tested with an intertrial interval (ITI) of ~ 10 min and received five daily trials for a period of five days. Statistical analysis for behavior was carried out using STATISTICA (Dell Software) where effect of genotype and time on distance traveled and percent correct choices were analyzed using ANOVA, with repeated measure of time followed by Newman-Keuls *post hoc* analysis when appropriate.

Supplemental Material References:

Colonnese MT, Khazipov R (2010) "Slow activity transients" in infant rat visual cortex: a spreading synchronous oscillation patterned by retinal waves. J Neurosci 30:4325-4337.

Csicsvari J, Hirase H, Czurko A, Mamiya A, Buzsaki G (1999) Oscillatory coupling of hippocampal pyramidal cells and interneurons in the behaving Rat. J Neurosci 19:274-287.

Gray EG, Whittaker VP (1962) The isolation of nerve endings from brain: an electron-microscopic study of cell fragments derived by homogenization and centrifugation. J Anat 96:79-88.

Karlsson RM, Hefner KR, Sibley DR, Holmes A (2008) Comparison of dopamine D1 and D5 receptor knockout mice for cocaine locomotor sensitization. Psychopharmacology (Berl) 200:117-127.
Mitchell RM, Janssen MJ, Karavanova I, Vullhorst D, Furth K, Makusky A, Markey SP, Buonanno A (2013) ErbB4 reduces synaptic GABAA currents independent of its receptor tyrosine kinase activity. Proc Natl Acad Sci U S A 110:19603-19608.
Petralia RS, Wenthold RJ (1999) Immunocytochemistry of NMDA receptors. Methods Mol Biol 128:73-92.
Traynelis SF, Dingledine R (1988) Potassium-induced spontaneous electrographic seizures in the rat hippocampal slice. J Neurophysiol 59:259-276.
Tricoire L, Pelkey KA, Daw MI, Sousa VH, Miyoshi G, Jeffries B, Cauli B, Fishell G, McBain CJ (2010) Common origins of hippocampal Ivy and nitric oxide synthase expressing neurogliaform cells. J Neurosci 30:2165-2176.